Young rift kinematics in the western Gulf of Aden: the Tadjoura-Ghoubbet extensional linked system, (Djibouti).

Mohamed A. Daoud[1], Bernard Le Gall[2], René C. Maury[2], Philippe Huchon[3], Hervé Guillou[4]

[1]Institut des Sciences de la Terre, Centre d'Etudes et de Recherches de Djibouti, B.P. 486, Djibouti Ville, Djibouti.
[2]Université Européenne de Bretagne, Université de Brest, CNRS; UMR 6538 Domaines Océaniques, IUEM, place N. Copernic, 29280 Plouzané, France.
[3]UPMC Université de Paris 6, CNRS; UMR 7193, ISTeP, 4 place Jussieu 75252, Paris Cedex 05, France.
[4]UMR 1572, LSCE/CEA-CNRS, Domaine du CNRS, 12 avenue de la Terrasse, 91118 Gif-sur-Yvette, France.

Résumé

En prenant les Basaltes du Golfe (2.8-1.1 Ma) comme marqueurs tectoniques du rift Tadjoura, et en combinant les données morphologiques disponibles (topographiques et bathymétriques), la structure générale du rift Tadjoura est assimilée à celle d'un hémi-graben à vergence sud, d'environ 20 x 30 km, bordé au Nord par un système de failles bordières et passant au Sud à une marge flexurée impliquant un substratum volcanique (séries des traps du Dalha et Somalis). Sur la base de données géochimiques et géochronologiques (méthode KAr), l'organisation volcano-stratigraphique ainsi que les caractéristiques géochimiques des séries basaltiques de la marge sud ont été affinées, avec notamment la mise en évidence d'un nouveau complexe intrusif (dyke-sill), l'ensemble de Goumarre, daté à 2.4-1.7 Ma, qui alimente trois chapelets d'édifices volcaniques alignés au N80°E, parallèlement à l'axe du Golfe. Les séries basaltiques concernées (Golfe, Somali, Goumarre et volcan Hayyabley) présentent une signature géochimique de basaltes transitionnels à affinité thôleiitique, excepté ceux du volcan Hayyabley, plus appauvris et aux caractéristiques géochimiques particulières.

L'hémi-graben de Tadjoura est la première expression tectonique du rifting (à polarité Golfe d'Aden) à travers la province magmatique Afar, et il correspond à une extension cumulée estimée à 25-30%. Le rajeunissement progressif des structures extensives vers la partie centrale de l'hémi-graben témoigne de la concentration de la déformation dans l'axe, sismiquement actif, du dispositif.

L'analyse morphostructurale, géométrique et statistique des systèmes de failles extensives exposées sur les marges du rift, au niveau de la zone Tadjoura-Obock au Nord, et de la Plaine de Djibouti au Sud, permet en particulier de démontrer la plus grande complexité du dispositif faillé méridional qui se marque par (i) la présence de structures extensives transverses N140°E et (ii) de grandes variations latérales du style tectonique. Celles-ci témoignent d'un gradient croissant de la déformation vers l'Ouest, en direction d'une discontinuité transverse, la

zone d'Arta. A l'inverse des modèles cinématiques précédents qui interprétaient ce couloir décrochant subméridien comme partie intégrante du système transformant de Maskali, la zone d'Arta est considérée dans ce travail comme une structure héritée, à polarité Mer Rouge, qui entrave la propagation axiale, vers l'Ouest, des structures extensives du système Golfe d'Aden. Ce blocage frontal de la déformation provoque le saut du rift vers le Sud Ouest, depuis le Golfe de Tadjoura vers la zone du Ghoubbet, selon un modèle de type 'hard linkage', en opposition avec les conceptions précédentes qui favorisaient un transfert du rifting par l'intermédiaire

Mots-clés : Afar, rift de Tadjoura, ext

Abstract

The Tadjoura rift forms the westernmost edge of the western Gulf of Aden Sheba ridge, between Arabia and Somalia as it enters into the Afar depression. From structural and remote sensing dataset, the Tadjoura rift is interpreted as an asymmetrical south-facing half-graben, about 40 km wide, bordered by a large to the north. It is partially filled by old (Oligocene?) to recent (Quaternary) sediments which onlapped the rift shoulder. Basalts along its shallower southern flexural margin. The major and trace element analysis of 78 young onshore lavas allows us to distinguish and map four distinct basaltic types, namely the Gulf, Asal-Ghoubbet, Arta, and Tadjoura basalts. These results

We date several distinct episodes of onshore extensional fault populations show marked changes in structural styles along strike, in all direction parallel to the rift axis. These fault disturbances are assigned to the arrest of propagation against pre-existing discontinuities, namely the Arta transverse zone. Accordingly, we suggest that the present-day offset jump of rifting into the Asal-Ghoubbet rift segment results from structural inheritance, in contrast with the *en échelon* or transform mode of deformation that prevailed along the entire length of the Gulf of Aden extensional system.

Afar, Tadjoura rift, active/recent extension, faults, basalts, [illegible]

The segmentation of rift/ridge systems is controlled by several physical parameters which interact at various scales of times and space, and usually lead to intricate geometrical configurations. The large-scale spatial architecture of a propagating rift is known to depend merely on the absolute motions of the lithospheric plates, and on major heterogeneities in the strength of either the brittle crust (e.g. inherited structures), or the lower crust (e.g. partial melt zones) (*Ziegler and Cloetingh*, 2004; *Wijns et al.*, 2005). At a smaller scale, the segmentation of

the spreading axis within the rifted zone itself is commonly assigned to (i) its obliquity to the extension direction, and (ii) the angle between the axis of individual rift segments and the general trend of the rifted zone (*Abelson and Agnon,* 1997). The resulting complex multi-scale rift architecture is typically expressed along the Sheba westerly-propagating rift-drift system (Eastern Afar) by two nearly orthogonal first-order arms that, in turn, display specific segmented axial patterns (Figure 1A-B). Along most of its EW-trending path, the Sheba oceanic ridge is systematically offset to the southwest. This offset occurs through either a left-stepping ridge-transform network (up to the Shukra El Sheikh discontinuity, e.g. *Manighetti et al. 1997*) or oblique transfer zones with onlapping fault networks, up to the Tadjoura rift (TR) to the west (Figure 1B) (*Cochran,* 1981*; Tamsett and Searle,* 1988*; Manighetti et al.*, 1997*; Dauteuil et al.*, 2001). There, the nearly EW-trending axis veers abruptly counter-clockwise into the N120°E-oriented Ghoubbet rift, which is part of a subaerial, and partly emerged, rifted zone encompassing to the north the Asal and Manda Inakir *en echelon* subrifts (Figure 1B) (*Manighetti et al., 1998*). The structural link between the two sub-orthogonal rift arms in the TR has been variously interpreted as [illegible] the Tadjoura-Asal-Ghoubbet transform fault (Figure 1B) (*Cochran,* 1981*; Tamsett and Searle,* 1988*; Arthaud et al.*, 1980*; Gaulier and Huchon,* 1991) or to an overlapping rift zone enclosing a network of en echelon [illegible] (*Manighetti et al.*, 1997).

The goal of the present work is to address the mechanical [illegible] transfer between the Tadjoura and Ghoubbet rifts, with emphasis on the structure of the TR. Our study integrates (i) available [illegible] and bathymetric offshore data, (ii) sampling, geochemical analysis and [illegible] of young basalts from the [illegible] and (iii) [illegible] based on field studies and remote sensing [illegible]

The [illegible] displays a half-graben structure, which [illegible] progressively shifts southwestwards towards its inner part during the last 3 Ma. In addition, we propose that submeridian [illegible] inherited from the early stage of rifting in the Afar transverse zone (Figure 1B) may have locked the westerly propagation of extension in the TR, hence causing the jump of rift axis southwestwards into the Ghoubbet sub-rift.

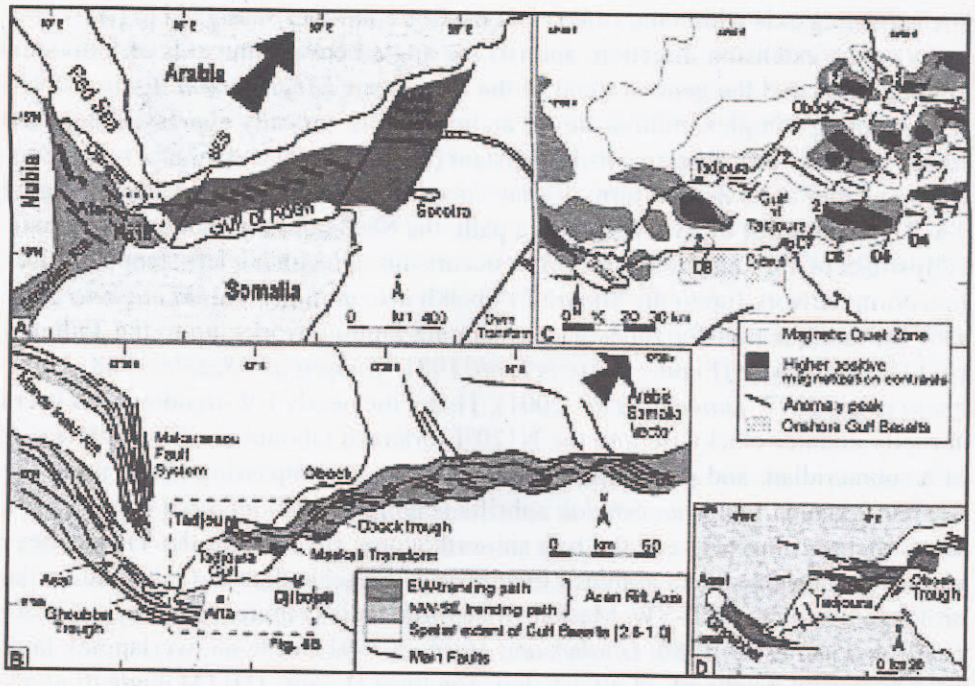

Figure 1: Various types of rift segmentation along the Gulf of Aden plate boundary between Arabia and Somalia. The active EW-trending Gulf of Aden (Sheba) rift-drift system evolves westwards into the sub-orthogonal Ghoubbet-Asal and Manda Inakir rifts. (A). Plate kinematic setting of the Afar Triple Junction. Thick arrows represent plate motion vectors, and the box indicates the study area. (B). Main physiographic features of the western Gulf of Aden rift system, modified from *Manighetti et al.* (1997). The revised spatial extent of onshore Gulf Basalts, as well as the Arta transverse zone (shown as the white NS domain centered on the Arta locality) are shown. (C). Aeromagnetic map of the Tadjoura Gulf, from *Manighetti et al.* (1997), with modified onshore parts. Dashed lines (D_{1-8}) represent transform faults offsetting magnetic segments. Numbers refer to specific magnetic anomalies. (D). 'Overlapping subrift' model developed by *Manighetti et al.* (1997) to account for the relationships between the Tadjoura and Ghoubbet rifts. The inner floors of the rifts are shaded

Methodology

The 3D-structure of the TR was first investigated in map-view, and along selected cross-sections, by merging onshore geology with existing offshore data, which include bathymetric maps (*Audin*, 1999; *Dauteuil et al.*, 2001) and analog, single channel seismic reflection profiles acquired during the TADJOURADEN cruise in 1995. The deep geometry of a number of offshore faults has been determined using the TADJOURADEN seismic reflection profiles. Onshore field studies have been focused on poorly investigated areas from the southern margin of the TR, e.g. the Djibouti Plain, and the Arta transverse zone, where >3 Ma old volcanics are widely exposed (Figure 1B). Quantitative analysis of fault parameters (length, azimuth, spacing) was conducted on fault populations extracted from ASTER

satellite images (lateral resolution 15 m) and corresponding digital elevation models (vertical resolution 7 m). Estimates of vertical displacement along each fault were derived from fault scarp geometry. Seriated topographic profiles across each individual fault scarp gave the maximum value of displacement at the surface. The age pattern of faulting within the TR was established from cross-cutting relationships of faults with [illegible] volcanic and sedimentary sequences.

[illegible] analyses (major and trace elements) and radiometric dating (K/Ar method) have been focused on [illegible] several basaltic units and mapping them. Major [illegible] on bulk rocks were [illegible] spectroscopy. Relative [illegible] for SiO2, and ~2 % for other major [illegible] (except for MnO (~0.01 %), and ca. 5% for trace elements. The analytical techniques are described in *Cotten et al.* (1995). Ar isotopic compositions and K contents of two samples (Table 2) were measured at LSCE, Gif sur Yvette and ISTEEM, respectively. Ar analyses were performed using the unspiked technique procedures detailed in *Hurtmen et al.* (2002) and *Gaillou et al.* (2004). Ages were calculated using the constants recommended by Steiger and Jäger (1977).

Spatial and temporal distribution of synrift volcanism in the Tadjoura rift

General rift setting

The Sheba ridge within the Gulf of Aden forms, together with the Red Sea and the Ethiopian rift, the three diverging branches of the Afar triple junction (Figure 1A). According to magnetic anomaly data, mid-oceanic ridge segments and fracture zones initiated along the eastern part of the [illegible] (*Manighetti et al.*, 2006), or possibly at 20 Ma (*Courtillot et al.*, in press), and then propagated westwards conjugately to the N40°E direction of Arabia-Somalia plate separation (*Cochran*, 1981) (Figure 1A). Emplacement of incipient oceanic crust at the western tip of the Sheba ridge is recorded [illegible] Gulf of Tadjoura by ~2 Ma-old paired magnetic anomalies (Figure 1C). The anomalies partly coincide with the 3-1 Ma Gulf basaltic series which floor the Tadjoura Gulf, and outcrop onshore in its northern (Tadjoura) and southern (Djibouti Plain) margins (*Manighetti et al.*, 1997) (Figure 1B). The EW-oriented TR-related structures intersect at high angle older tectono-magmatic fabrics displaying a submeridian orientation in the Mabla (15-11 Ma), Somali (7.2-3.6 Ma), and Ribta (3.6 Ma) substratum series, emplaced at an earlier stage of rifting.

The Gulf Basalts are a potentially accurate structural marker of the rift history recorded by the TR in the last 3 Ma, and it is therefore important to determine their spatial and temporal distribution for a better definition of the TR. That has

been attempted by using new geochemical and age dataset obtained on basaltic units in the Djibouti Plain, i.e. on the southern margin of the TR. Combined with previously published K-Ar ages, this dataset allows us to discriminate four recent basaltic units, i.e. the Gulf, Somali, Goumarre, and Hayyabley Basalts, hence allowing significant revision of the 2D-map structure of the TR (Figure 2A). Finally, although they are younger than the Gulf and Somali Basalts which they crosscut, the Goumarre basalts were not recognized as a distinct type prior to this study.

Geochemical characteristics of the Tadjoura rift basalts

Sampling and classification.

Several main lava units have been analyzed for major and trace elements (see Table 1 for representative analyses). They include 24 samples from the Gulf Basalts in the Djibouti Plain, 10 from the same unit north of the Tadjoura Gulf, 22 from the Somali Basalts, 16 from the young volcanic cones and intrusions of the Goumarre Basalts, and finally 9 from the Hayyabley Volcano. We have shown in envelopes in Figures 3A–D, the fields of previously published analyses of (1) the [illegible] et al., 1994), (2) the Asal Basalts (*Richard, 1979*; *Joron et al., 1980*; *Vidal et al., 1991*; *Deniel et al., 1994*), and (3) Afar Stratoid basalts (restricted to the [illegible] *et al., 1990*; *this study*).

Figure 2. Revised geological sketch map of the onshore parts of the Tadjoura rift. (A) Revised map showing the distribution of the various basalt types and the location of dated basaltic rocks. Ages in MY (numbers inside the squares) from published and unpublished data. (B) Location of the main structural features mentioned in the text. (C) Location of the studied area.

regression is not clearly observed.

All the collected samples are basalts, according to the total alkalies-silica (TAS) classification scheme of *Le Bas et al.* (1986). In the TAS plot of Figure 3A, they lie on both sides of, but close to, the line separating the fields of subalkalic and alkalic basalts (*Irvine and Baragar*, 1971), with the exception of Hayyabley Basalts which are clearly subalkalic. The Gulf, Goumarre and Somali Basalts can therefore be considered as transitional basalts with a dominant tholeiitic tendency (*Richard*, 1979; *Bizouard and Richard*, 1980; *Joron et al.*, 1980a,b; *Vidal et al.*, 1991; *Deniel et al.*, 1994). The various groups may be quite readily distinguished using the TAS plot (Figure 3A), which has been used, together with other major and trace element data (Figures 3B-D) to draw the boundaries between them in the new geological sketch map (Figure 2A). Indeed, the Somali Basalts are more silica-rich than the others (SiO_2: 48-52 wt.%), while Hayyabley Basalts are consistently depleted in alkalies ($Na_2O + K_2O \sim 2$ wt.%), and the Goumarre Basalts are, at equivalent SiO_2 contents, richer in alkalies than the Gulf Basalts. Among the latter, the compositions of samples collected on both sides of the Tadjoura Gulf systematically overlap, as already noted by *Richard* (1979), *Bizouard and Richard* (1980), and *Gasse et al.* (1983).

Major and trace element features

Selected plots of major and transition elements against total iron as FeO versus MgO ratios (FeO*/MgO) are shown in Figure 3B. Once again, the Hayyabley Basalts (*Daoud et al.*, 2010) differ from all the other groups by their more primitive character (lower FeO*/MgO ratios, higher Ni concentrations), and their much lower TiO_2 and P_2O_5 contents. Gulf Basalts tend to display lower FeO*/MgO ratios (1.5 to 2.5) than the Goumarre and Somali Basalts (2 to 3), as well as lower SiO_2 (45-48 wt. %), TiO_2, P_2O_5 and K_2O contents. Regarding the transition element Ni and others not shown (Co, Cr), they are intermediate between the relatively primitive Hayyabley Basalts and the evolved Goumarre and Somali Basalts.

The envelopes of the incompatible multi-element patterns of the studied basalts, normalized to the Primitive Mantle (*Sun and McDonough*, 1989) are shown in Figure 3C. While Hayyabley Basalts have flat to slightly depleted patterns, the Gulf, Goumarre and Somali Basalts display moderately enriched patterns, typical

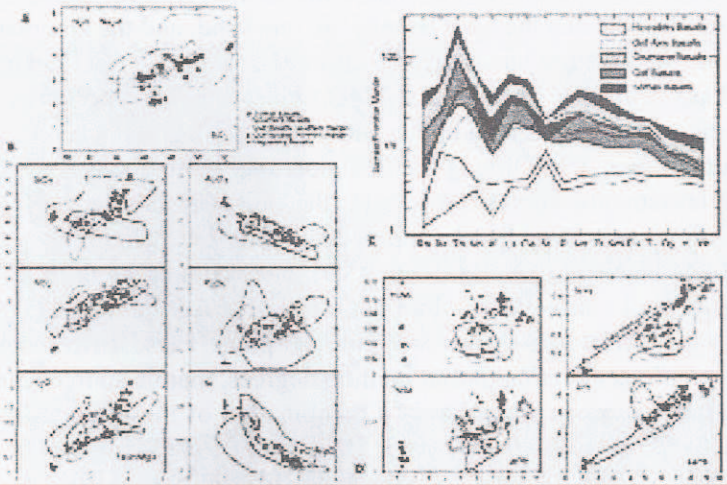

three groups. Basically, all ratios using an element plotting to the left or the middle of the multi-element plot (e.g. Th, Ba, Nb, La, Zr or others not shown like Rb, K, Ce, Sr, P) *versus* an element plotting to the right (Y, Yb) may be used to distinguish the moderately enriched Gulf Basalts from the more enriched Goumarre and Somali Basalts. These geochemical plots, together with geomorphological, structural and age data, led us to shift the map limit between the Gulf and Somali Basalts in the Djibouti Plain 10 km further north than drawn on previous maps (*Gasse et al.*, 1983, 1986). In addition, the abrupt chemical change observed at a depth of 220 m in basalts drilled in the PK20 borehole (Figure 2A) is consistent with the transi-

from the upper Gulf Basalts to the underlying Somali Basalts. Some of the differences observed between the Gulf Basalts, on one hand, and the Goumarre and Somali Basalts, on the other hand, may be attributed to olivine fractionation. Indeed, the latter basalts display higher FeO*/MgO ratios, lower Ni and other compatible transition element contents, and higher SiO_2, TiO_2, P_2O_5 and K_2O contents than the Gulf Basalts (Figure 3B). Olivine fractionation might also account for their higher incompatible element contents compared to the Gulf Basalts (Figure 3C). However, as this process does not fractionate appreciably ratios between highly incompatible elements (e.g. Th/Nb and Th/Ba, Figure 3D), nor strongly modifies the shapes of REE patterns (and consequently the La/Yb ratios; *Allègre et al.*, 1977), it cannot account for the differences shown in Figure 3D plots. These differences might result from variations affecting partial melting degrees, mantle source heterogeneity, crustal contamination, or more likely a combination of these processes (*Joron et al.*, 1980a, b; *Barrat et al.*, 1990, 1993; *Vidal et al.*, 1991; *Deniel et al.*, 1994). In addition, the different La/Yb ratios of the Goumarre and Somali Basalts, which display nearly equivalent enrichments in most incompatible elements, might indicate that the former derive from a deeper (i.e. garnet-bearing) mantle source than the latter, as garnet incorporates selectively heavy REE.

Spatial

(Figure 2A).

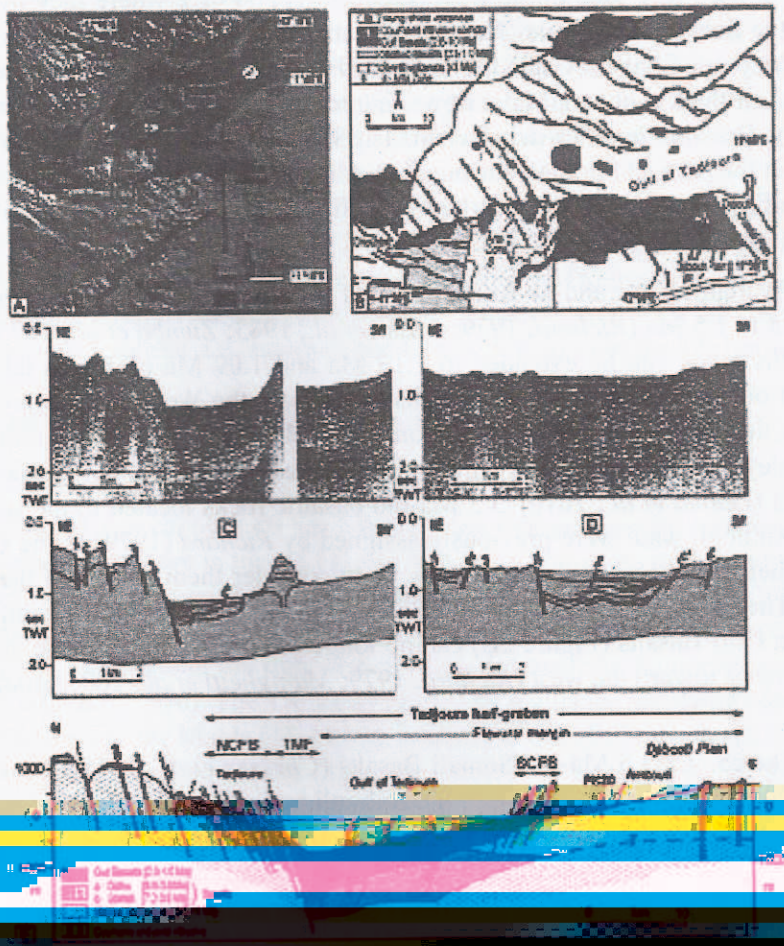

Overall structure of the Tadjoura rift. (A). Topographic and bathymetric contour map (from *Audin, 1999*, modified) and ASTER digital elevation model. Dashed lines represent the Maskali transform (MT) and the Bour Ougoul transverse fault systems. Note the strong NS-oriented structural grain in the Arta zone. The traces of the structural cross-section in Figure 2E and the two interpreted seismic profiles in Figures 2C and D are shown. HV, Hayyabley volcano. (B). Structural map of the TR obtained (i) by merging onshore geology with offshore bathymetric data, and (ii) by using the Gulf Basalts as a stratigraphic marker (only drawn onland). ATZ, Arta transverse zone; HV, Hayyabley Volcano; NCFB and SCFB, Northern and Southern coastal fault belts, respectively. (C) and (D), Raw (top) and interpreted (bottom) TADJOURADEN offshore seismic profiles (time-sections) perpendicular to the NW-SE-oriented fault-controlled Tadjoura inner trough (see traces in Figure 4A). (E). Interpretative structural cross-section showing the Tadjoura rift as a south-facing half-graben, partly filled up by Gulf Basalts. The elements of the deep structure of the Tadjoura rift are conjectural. The geometrical relationships between the underlying Somali and Dalha basalts are extrapolated from patterns observed onshore along the Bour Ougoul lineament on the NW flank of the Ali Sabieh antiform (see Figure 4A for location).

The Gulf Basalt pile reaches a maximum thickness of 220 m in boreholes drilled in the PK20 area to the west (Figures 2A and 4E), where they overlie the top of the Somali Basalt pile. The uppermost sequence of Gulf Basalts is exposed in the Ambouli-Chabelley area to the south (Figure 4E). It includes a succession of thin (<1 m-thick) subaerial lava flows, interdigitated with conglomeratic alluvial horizons (basaltic boulder-rich facies). The latter probably derived from uplifted reliefs in the Arta and Somali surrounding domains. The young and flat-lying Gulf Basalts flows onlap previously tilted Somali Basalts along the Ambouli flexural zone (Figure 4E).

Available K-Ar and Ar-Ar ages of Gulf Basalts from the Djibouti Plain range from 2.8 to 1.5 Ma (*Richard*, 1979; *Gasse et al.*, 1983; *Zumbo et al.*, 1995; Figure 2A). This range can be extended to 1.19 Ma and 1.09 Ma (Table 2) taking into account our new results on Gulf Basalts flows from the Wea paleo-valley (Figure 2A). In the Warabor wadi cross-section, the Gulf Basalts pile is overlain by the Hayyabley volcano lava flows which yielded ages of 1.06 ± 0.09 Ma and 0.93 ± 0.06 Ma (*Daoud et al.*, 2010). 3.3 Ma-old basaltic rocks located to the south-east of the Ambouli wadi were previously assigned by *Richard* (1979) to the Gulf Basalts. Their geochemical features allow us to consider them as part of the Somali series. Therefore, the revised longitude *versus* age plots drawn for the southern and northern Gulf Basalts (Figure 2B) can no longer be used to support the idea of an age decrease toward the west (*Richard*, 1979; *Manighetti et al.*, 2001; *Audin et al.*, 2004).

The ca. 7.2-3.0 Ma-old Somali Basalts (*Chessex et al.*, 1975), which cover most of the Djibouti Plain south of the Ambouli regional-scale flexure, form a monotonous and weakly incised plateau (Figures 4A, B, and E). They likely represent a trap-like pile, similar to the nearby Central Afar Somali Basalts (see *Barberi et al.*, 1975; *Varet*, 1975; *Zumbo et al.*, 1995). In the Ifoubol area (Figure 2A), the Somali Basalts rest unconformably over tilted and partially eroded rhyolitic sequences of the 15-11 Ma-old Mabla series (*Zumbo et al.*, 1995).

With regard to the Goumarre volcanoes, which punctuate the Djibouti Plain [illegible] parallel arrays of basaltic vents crosscutting the Somali lavas, and referred here as to the Goumarre Basalts (from their type-locality, i.e. the Goumarre strombolian lapilli/ash cone, dated at 1.75 Ma by *Gasse et al.*, 1983). These volcanic corridors, each of them a few km-wide, are sharply cut to the east by the [illegible] to the west, their tips remain within the Somali Basalts and do not reach the older substratum series of the Ali Sabieh range. In addition to numerous small strombolian or maar-type volcanoes, with maximum height of ca. 100 m, the Goumarre Basalt series includes various types of intrusions (dikes, sills, plugs), often spatially connected with these volcanoes. The genetic relationships between Goumarre-type [illegible] can be observed on aerial photographs

the Dey Dey central corridor in the Goumbourta Atar strombolian cone area (Figure 2A). There, lava flows seem to either radiate from small-scale vents, or diverge on both sides of N80°E-trending fault/fissure structures which correlate in the field with narrow (1-2 m-thick) dykes and thicker (15 m) sills crosscutting the Somali Basalts. Most of the Goumarre Basalts are therefore likely to have been emitted from transverse fault/dyke corridors, nearly parallel to the present-day Gulf axis. Published radiometric ages from the Goumarre (24.3 ± 1.84 [1SD] Ma) and

SSW. Its inner and deeper part is occupied by the Tadjoura trough, which is bounded to the north by a prominent fault system, including the Tadjoura master fault, and its highly faulted footwall block, partly exposed in the NCFB. To the south, a ca. 20 km-long typical flexural margin shallows gradually southwards, up to the Djibouti Plain, where Gulf Basalts are locally dissected by a high density antithetic fault system in the SCFB. The flexure is locally punctuated by shield volcanoes.

The deep structure of the Tadjoura inner trough is constrained down to about 2 s (two-way travel-time), or depth of 4-5 km, by selected single-channel seismic reflection profiles striking NE-SW, orthogonal to the prominent [illegible]

1.2 km, and 90% of length values less than 2.8 km (Figures $6A_{2-3}$). Fault population is homogeneously distributed, but with a marked increase of fault spacing westwards (Figure $6A_4$). Individual faults are clustered into 4 to 5 major faults facing the south, and causing the downwarping of the Gulf Basalts towards the gulf axis. Very few antithetic structures, with minor associated displacement, do occur (e.g., F_{80} in Figure 5B). Along-strike variations of individual fault profiles are observed on the three orthogonal cross-sections shown in Figure 5B. The horizontal surface of most individual footwall blocks suggests non-rotational structures. The largest throw values (>50 m) systematically occur along the oldest (pre-alluvium) faults to the north. However, estimates of throws along the youngest (post-alluvium) faults to the south might be underestimated because of syn-faulting alluvial screes at the foot of some fault scarps. Vertical throw in the oldest fault network to the north increases markedly southwards from 65 m (F_6), 100 m (F_4) to >130 m (F_8). A comparison of the three topographic sections shows that the total fault-induced elevation slightly decreases westwards from 310 m (section 1) to 280 m (section 2), and to 200 m (section 3).

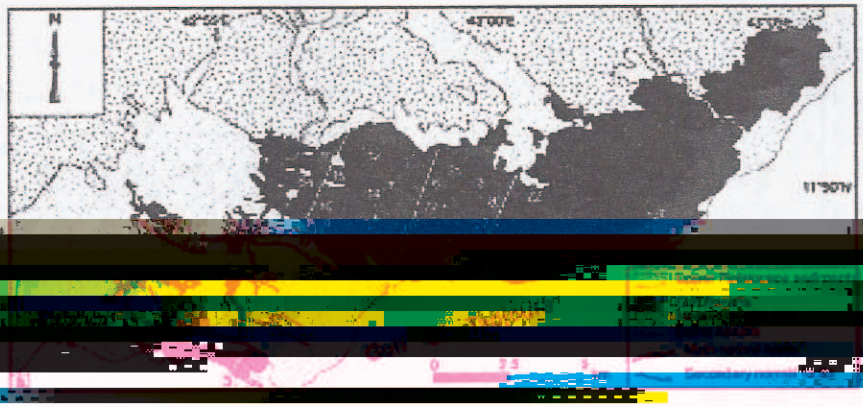

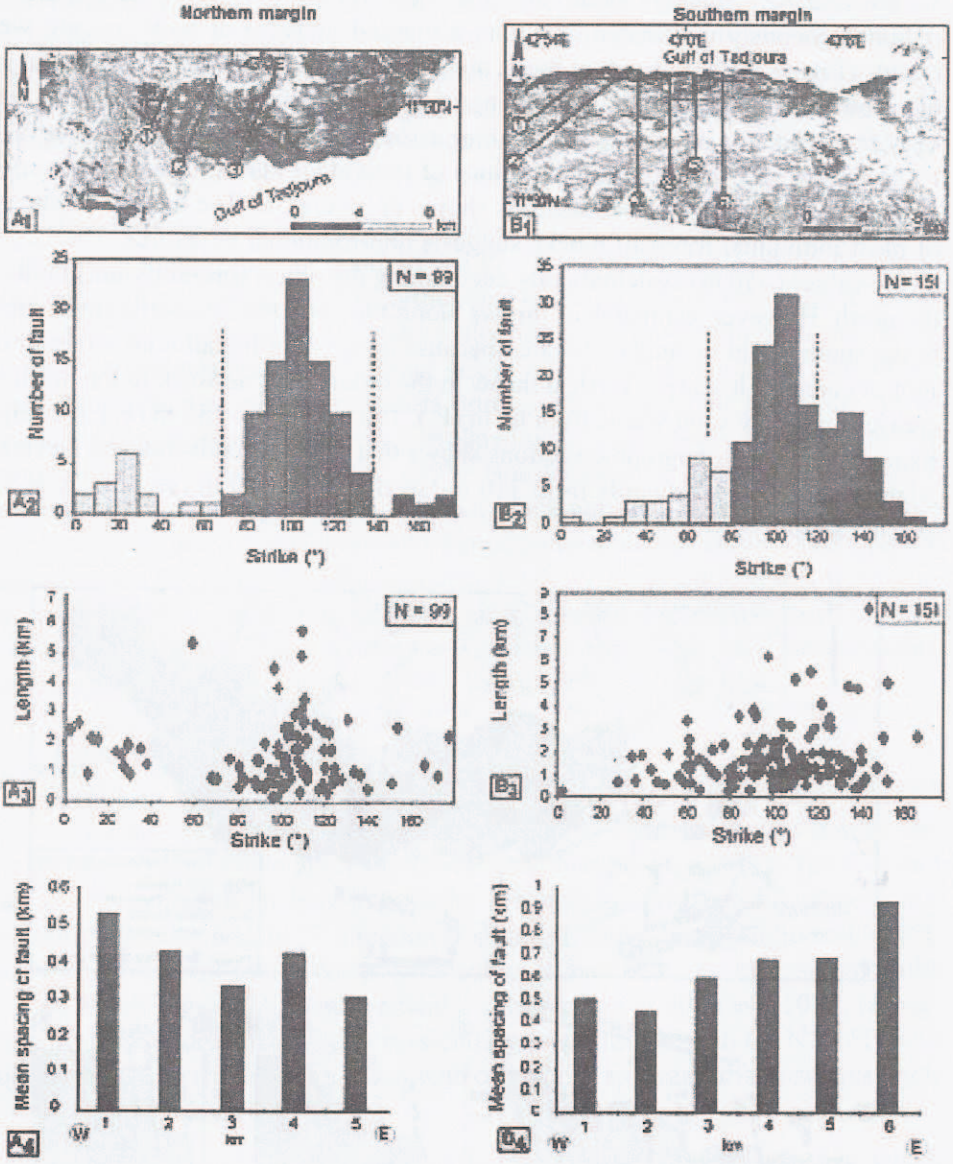

Figure 6: Geometrical and statistical characteristics of extensional fault networks in the North (A, left panel) and South (B, right panel) Coastal Fault Belts. (A$_1$, B$_1$), [illegible]; (A$_2$, B$_2$), histograms of fault strike; (A$_3$, B$_3$), average south to fault strike regularly spaced [illegible] (A$_4$, B$_4$), [illegible] (length) North to South [illegible] (trace) [illegible] (CCW).

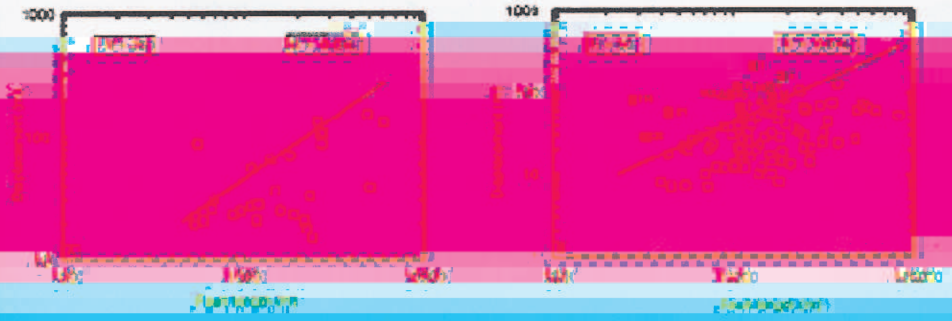

Figure 7. Log-log plot of maximum fault displacement versus fault length for structures in the North (7A) and South (7B) Coastal Fault Belts. The straight line corresponds to the best-fit correlation ($D=0.04L$). Empty and filled symbols denote unrestricted and restricted (over-displaced) faults, respectively. In Figure 7B, ten out of twelve over-displaced faults are located close to the Arta zone. Corresponding fault numbers are identical to those shown on Figure 6A.

These along-strike variations of cumulate fault displacement are illustrated by the distribution of throw along some individual structures, such as faults labelled [illegible] close to the [illegible]

The cumulative bulk [illegible] the fault system (Figure 6A) [illegible] mean fault dip of 60°-70°, similar to those reported elsewhere in the Afar depression [illegible] 1994). The bulk extension decreases regularly from 3.4% to 1.6% westwards. Special attention has been paid to the displacement-length ratio (D/L), which may supply information about fault growth [illegible] *et al.*, 199[illegible] *Manighetti et al.*, 2001), as a function of either the [illegible] unrestricted [illegible] the faults (*Watterson*, 1986; *Gillespie et al.*, 1992), or the [illegible] *Wojtal*, 1996). D refers to maximum displacement and L to fault trace length in map [illegible] growth models predict that displacement is maximal at or near the centre of the fault and decreases toward its tips (*Cowie and Scholz*, 1992). It is also generally accepted that the scaling relationship between L and D is :

$$D = cL^n$$

where c is a constant and n is a scaling exponent, ranging from 0.5 (*Fossen and Hesthammer*, 1997) to 1.5 (*Walsh and Watterson*, 1988; *Gillespie et al.*, 1992; *Dawers et al.*, 1993; *Schlische et al.*, 1996). When n = 1, a commonly accepted [illegible]

[illegible] earth unit. For a linear scaling law (i.e. n=1), c is simply the D/L ratio which characterizes the fault population. In the log-log plot of maximum fault displacement versus length, *Schlische et al.* (1996) have defined a best-fit linear curve with [illegible] 0.03). *Manighetti et al.* (2001) [illegible]

along fault systems in the Afar region is related to their time-space growth and propagation history, and they proposed a best-fit linear curve with $D=0.04L$. These authors indicated that the maximum D/L values are characteristic of restricted faults which plot above the $D=0.04L$ line, while unrestricted faults plot below this line. In the present work, the D/L ratios calculated for N100°E faults (29 data) are in the range 0.0062 - 0.15, and thus plot below or along the line $D=0.04L$ (excepted one biased value due to measurement error) (Figure 7A). In agreement with the model of *Manighetti et al.* (2001), this feature indicates that the N100°E extensional fault

Figure 8. Map distribution and morphostructural expression of the extensional fault pattern in the South Coastal Fault Belt. (A). Structural map from ASTER remote sensing data interpretation. White lines are the traces of the seven topographic cross-sections shown in Figures 8B (profiles 1 to 4) and 9B (profiles 5 to 7). (B). Morphostructural NS-trending cross-sections showing increasing structural complexity towards the Arta zone to the west.

The SCFB fault network displays a much more intricate organisation than that described above for the NCFB conjugate margin (Figure 8A). It includes three distinct sets of faults at N100-110°E, N130-140°E, and to a lesser extent N60-70°E (Figure 6B$_2$). The dominant N100°E antithetic fault pattern (with respect to the

nantly left-lateral slip along N140°-trending structures (Figure 9A) (*Lépine et al.*, 1980; *Lépine and Hirn*, 1992). Several NW-SE transverse faults extend further to the SE, onshore, through the Gulf Basalts which cap the SCFB (Figure 9A). There, they form isolated and segmented structures, locally outlined by a dense swarm of small volcanic vents, ~1 Ma old (*Gasse et al.*, 1983). They show a longer and more linear map trace than the Gulf-parallel faults, with which they usually merge. Transverse faults dip consistently towards the NE, and their cumulate extensional displacement increases regularly towards the Arta zone, in association with the ca. 300 m elevation of the topography (Figure 9B). Extensional scarp heights measured along the major NE-facing faults gradually increase westwards from 20 m and 50 m (profile 7), to 70 m and 80 m (profile 6), and lastly 70 m, 30 m and 90 m (profile 5). The *D/L* ratios calculated for transverse faults (21 data) are in the range 0.0056-0.022, i.e. lower than those of the Gulf-parallel faults. The low *D/L* ratios indicate a deficit of vertical displacement with respect to fault length, as typically documented during fault growth processes dominated by linkage where fault length increases without increasing height (*Cartwright et al.*, 1995). This feature is consistent with the isolated, linear and linked characteristics of the transverse faults cited above.

The sketch structural map in Figure 9A shows that very few transverse and Gulf-parallel TR-related faults crosscut the >3 Ma-old volcanic terranes forming the Arta zone. In this area, the 8.6-3.8 Ma-old Dalha Basalts and the overlying Ribta felsic lavas (3.6 Ma) are involved into a broad, 10 km-wide, upright arched structure, oriented N-S, i.e. nearly orthogonal to the E-W axis of the TR. This Arta anticline is in turn dissected by a dense network of NS-N20°E fault/fractures, parallel to the anticline axis and locally intruded by felsic bodies of the Ribta Fm. Most of these submeridian fractures were later reactivated as strike-slip faults (*Arthaud et al.*, 1980). From these structural relationships, the Arta anticline is inferred to have formed as a magma-driven structure overlying a felsic intrusion emplaced during the 3.6 Ma Ribta event.

Timing of faulting in the Tadjoura rift

The combination of published and new age determinations on both sedimentary and volcanic rift sequences exposed on the onshore margins of the TR supplies temporal constraints on the sequential development of the Tadjoura half-graben during the last 3 Ma. The Gulf-parallel extensional fault network in the two coastal belts shows a relatively clear age progression depicted on the NS cross-sectional diagram in Figure 10A. As already argued by *Manighetti et al.* (1997), two successive extensional fault sets are evidenced on the northern flank of the TR, i.e. in the NCFB. The most external faults are post-dated by 1.4-0.8 Ma-old alluvial fans (*Gasse*, 1991), while younger similarly-trending [illegible]

map-view, the TR rhomb-shaped structure involves a composite network of dominantly extensional faults, striking EW (Gulf-parallel) and NW-SE.

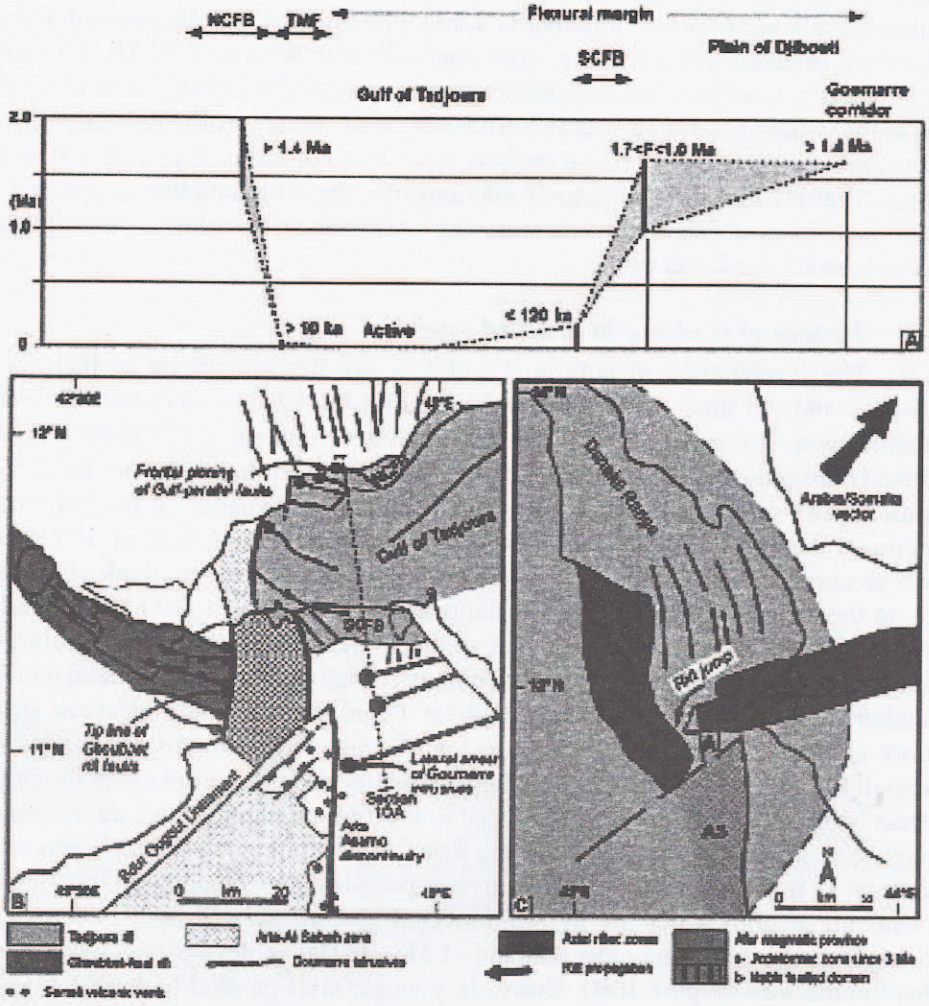

Figure 10: Kinematics of rift propagation throughout the Tadjoura-Ghoubbet connection zone. (A). Timing of faulting along a synthetic cross-section of the Tadjoura Rift. Despite age uncertainties, a pattern of younging of strain is observed from the margins to the inner part of the Tadjoura Rift, indicating progressive axial focusing of extension. NCFB: Northern Coastal Fault Belt; TMF: Tadjoura master fault; SCFB: Southern Coastal Fault Belt. (B). Rift kinematic model in the Tadjoura-Ghoubbet linkage zone, emphazing [illegible] subsidiary structures in the propagation of the Tadjoura rift. [illegible] showing a transitional [illegible] is transfer zone between [illegible] Afar magmatic province (the model of [illegible] Yemen are not considered). (C). Afar [illegible]

The latter trend occurs in the western termination of the TR at the longitude of ca 42° 45', i.e. in the northern offshore prolongation of the Arta zone. The TR-related faults which exclusively involve the Gulf Basalt-filled half-graben recorded a complex history within an overall westerly migration of tectonic activity (*Manighetti et al.*, 1997). The dating of fault-controlled volcanic activity (Quaternary)

Structural data suggest that strong submeridian terranes, including the Arta zone, transect orthogonally the western end of the TR (Figure 10B). To the south, these terranes extend towards the Ali Sabieh anticline (*Le Gall et al.*, 2010). They are bounded to the east by the so-called Arta-Asamo discontinuity, the > 60 km-long map trace of which is outlined by a variety of structures that indicate its long-lived history. To the north, the decrease of vertical motion along the NW offshore course of the N140°E transverse fault network (see Figure 4D) suggests the occurrence of a stronger substratum offshore the Arta zone. The strong mechanical behaviour of the Arta transverse zone during recent rifting is also confirmed by (1) the restricted location of earthquakes and aftershocks linked to the 1978 seismic crisis in the Tadjoura gulf (*Lépine et al.*, 1980; *Lépine and Hirn*, 1992; *Doubre*, 2004) (Figure 9A), and (2) the abrupt arrest of the EW-trending Ghoubbet rift fault network against its NS-trending western edge (Figure 10B).

Further south, the continuation of the Arta-Asamo discontinuity along the eastern flank of the Ali Sabieh anticline is deduced from the restricted distribution of the N80°E Goumarre fault-dyke corridors which do not penetrate westwards into the Ali Sabieh substratum series (Figure 10B). The inherited and deep-seated origin of the Arta-Asamo discontinuity is suggested by the NS alignment of Somali (7.2-3.6 Ma) volcanic vents along its inferred map trace (Figure 10B). This discontinuity might have been guided at depth by a large-scale Proterozoic fracture zone belonging to the Marda system (*Boccaletti et al.*, 1991).

During the recent SE Afar rift history, the Arta preexisting submeridian structures are therefore assumed to have provoked the frontal pinning of axial fault growth in the TR, and then the lateral jump of rifting in the Ghoubbet area, in response to inferred higher strength contrast, together with their orthogonal orientation to rift propagation. This abrupt change in rift kinematics probably occurred at ca. 900 ka, when diffuse volcanism and associated faulting started in the Asal-Ghoubbet rift (*Manighetti et al., 1998*; *Audin et al.*, 2001).

Conclusions

The major and trace element analysis of young basalts collected from onland Tadjoura Rift units (especially from the Djibouti Plain) allows us to distinguish four distinct types, namely the Gulf, Somali, Goumarre and Hayyabley Basalts. These results, together with new and previously published radiometric age data, lead us to propose a revised volcano-stratigraphic sketch map of the southern (SCFB) and northern (NCFB) margins of the TR. With respect to former studies (*Richard*, 1979; *Gasse et al.*, 1983, 1985, 1986), the Goumarre Basalts (2.46-1.69 Ma) are recognized as a distinct unit and the southern limit of the Gulf basalts in the Djibouti Plain is shifted ca. 10 km northwards. A consequence of this revision is that the progressive westerly younging of the Gulf Basalts suggested by previous authors (*Richard*, 1979; *Manighetti et al.*, 2001; *Audin et al.*, 2004) for the southern and northern borders of the TR is no more supported by the new longitude versus age trends for these basalts.

New structural data based on fieldwork and remote sensing analysis allow us to interpret the overall structure of the TR as an asymmetrical south-facing half-graben, about 35 km-wide, dominated by a large boundary fault zone to the north and extending southwards as a >20 km-long shallower flexural margin, partially exposed in the Djibouti Plain. There, it is locally disrupted by an antithetic southern coastal fault belt, and by the Goumarre transverse fault-dike corridors close to the inflexion point of the Somali Basalts monocline. Recent faulting is spatially restricted to the Gulf Basalts which form two narrow strips on the northern and southern margins of the TR.

The temporal change of the location of normal faults towards the inner trough of the half-graben indicates the progressive focusing of strain with time within the axial part of the rift. The geometrical and statistical analysis of onshore fault networks in the southern fault belt shows a westerly increase of [illegible] as-
[illegible]

- Barrat, J.A., Jahn, B.M., Joron, J.L., Auvray, B. & Hamdi, H. 1990. Mantle heterogeneity in northeastern Africa: evidence from Nd isotopic compositions and hygromagmaphile element geochemistry of basaltic rocks from the Gulf of Tadjoura and Southern Red Sea regions. Earth. Planet. Sci. Lett., 101, 233-247.
- Barrat, J.A., Jahn, B.M., Fourcade, S. & Joron, J.L. 1993. Magma genesis in an ongoing rifting zone: the Tadjoura Gulf. Geochim. Cosmochim. Acta, 57, 2291-2302.
- Bizouard, H. & Richard, O. 1980. Etude de la transition dorsale océanique/rift émergé: Golfe de Tadjoura, Asal, Afar central. Approche pétrographique et minéralogique. Bull. Soc. géol. Fr., XXII, 935-943.
- Black, R., Morton, W. & Rex, D.C. 1975. Block tilting and volcanism within the Afar in light of recent K/Ar date. In: Pilger, A., Rösler, A. (Eds.) Depression of Ethiopia. Schweizerbart, Stuttgart 1, 296-299.
- Boccaletti, M., Getaneh, A. & Bonavia, F. 1991. The Marda fault zone : a remnant of an incipient aborted rift in the paleo-African Arabian plate. J. Petroleum Geol., 14(1), 79-92.
- Cartwright, J.A., Trudgill, B.D. & Mansfield, C. 1995. Fault growth by segment linkage: an explanation for scatter in maximum displacement and trace length data from the Canyonlands Grabens of SE Utah. J. Struct. Geol., 17(9), 1219-1326.
- Cerling, T.E. & Powers, D.W. 1977. Paleorifting between the Gregory and Ethiopian rifts. Geology, 5, 441-444.
- Chessex, R., Delaloye, M., Muller, J. & Weidmann, M. 1975. Evolution of the volcanic region of Ali-Sabieh (T.F.A.I) in the light of K/Ar age determinations. In: Pilger, A., Rösler, A. (Eds.) Depression of Ethiopia. Schweizerbart, Stuttgart 1, 220-227.
- Cochran, J.R., 1981. The Gulf of Aden: structure and evolution of a young ocean basin and continental margin. J. Geophys. Res., 86, 263-287.705
- Cotten, J., Le Dez, A., Bau, M., Caroff, M., Maury, R., Dulski, P., Fourcade, S., Bohn, M. & Brousse, R. 1995. Origin of anomalous rare-earth element and yttrium enrichments in subaerially exposed basalts: Evidence from French Polynesia. Chem. Geol., 119, 15-138.
- Cowie, P.A. & Scholz, C.H. 1992a. Physical explanation for displacement-length relationship for faults using a post-yield fracture mechanics model. J. Struc. Geol., 14, 1133-1148.
- Cowie, P.A. & Scholz, C.H. 1992b. Displacement-length scaling relationship for faults using a post-yield fracture mechanics model. J. Struct. Geol., 14, 1149-1156.
- d'Acremont, E., Leroy, S., Maia, M., Patriat, P., Beslier, M.O. Bellahsen, N., Fournier, M. & Gente, P. 2006. Structure and evolution of the eastern Gulf of Aden: insigths from magnetic and gravity data (Encens Sheba Cruise). Geophys. J. Int., 165, 786-803.722
- Daoud, M.A., Barrat, J.A., Maury, R., Taylor, R.N., Le Gall, B., Guillou, H., Cotten, J. & Rolet, J. 2010. A LREE-depleted component in the Afar plume: further evidence from Quaternary Djibouti basalts. Lithos, 114, 327-336.
- Dauteuil, O., Huchon, P., Quemeneur, F. & Souriot, T. 2001. Propagation of an oblique spreading center: the western Gulf of Aden. Tectonophysics, 332, 423-442.
- Dawers, N.H., Anders, M.H. & Schloz, C.H. 1993. Fault length and displacement: scaling laws. Geology, 21, 1107-1110.
- de Chabalier, J.B. & Avouac, J.P. 1994. Kinematics of the Asal rift (Djibouti) determined from the deformation of Fieale volcano. Science, 265, 1677-1681.

- Deniel, C., Vidal, P., Coulon, C., Vellutini, P.J. & Piguet, P. 1994. Temporal evolution of mantle sources during continental rifting: the volcanism of Djibouti (Afar). J. Geophys. Res., 99, 2853-2869.
- Doubre, C. 2004. Structure et mécanismes des segments de rift volcano-tectoniques; études de *rifts anciens (Ecosse et Islande) et d'un rift actif (Asal-Ghoubbet). Unpublished Ph.D. Thesis,* Univ. du Maine.
- Fossen, H. & Hesthammer, J. 1997. Geometric analysis and scaling relations of deformation bands in porous sandstone. J. Struct. Geol., 19, 1479-1493.
- Fournier, M., Chamot-Rooke, N., Patriat, P., Petit, C., Huchon, P., Al-Kathiri, A., Audin, L., Beslier, M.O., d'Acremont, E., Fabbri, O., Fleury, J.-M., Khanbari, K., Lepvrier, C., Leroy, S., Maillot, B. & Merkouriev, S. (2010). Arabia-Somalia plate kinematics, evolution of the Aden-Owen-Carlsberg triple junction, and opening of the Gulf of Aden. J. Geophys. Res., in press.
- Furman, T., Bryce, J., Rooney, T., Hana, B., Yirgu, G. & Ayalew, D. 2006. Heads and tails: 30 million years of the Afar plume. In: Yirgu, G., Ebinger, C.J., & Maguire, P.K.H. (Eds.), The Afar volcanic province within the East African Rift System. Geol. Soc. London, Sp. Pub., 259, 95-119.
- Gasse, F. 1991. Tectonic and climatic controls on lake distribution and environments in Afar from Miocene to present. In: Katz, B. (Ed), Lacustrine Basin Exploration: Case studies and Modern Analogs. Am. Assoc. Petrol. Geol. Mem., 50, 19-41.
- Gasse, F., Fournier, M. & Richard, O. 1983. Carte géologique de la République de Djibouti, 1:100000. Djibouti. Notice explicative. ISERST, Ministère français de la Coopération, Paris.
- Gasse, F., Fournier, M., Richard, O. & Ruegg J.C. 1985. Carte géologique de la République de Djibouti, 1:100000. Tadjoura. Notice explicative. ISERST, Ministère français de la Coopération, Paris.
- Gasse, F., Varet, J., Mazet, G., Recroix, F. & Ruegg, J.C. 1986. Carte géologique de la République de Djibouti, 1:100000. Ali Sabieh. Notice explicative. ISERST, Ministère français de la Coopération, Paris.
- Gaulier, J.M. & Huchon, P. 1991. Tectonic evolution of Afar triple junction. Bull. Soc. géol. Fr., 162 (VIII), 451-464.
- Gillespie, P. A., Walsh, J. J. & Watterson, J. 1992. Limitation of dimension and displacement data from single fault and the consequences for data analysis and interpretation. J. Struct. Geol., 14, 1157-1172.
- Guillou, H., Singer, B., Laj, C., Kissel, C., Scaillet, S. & Jicha, B.R. 2004. On the age of the

éléments en traces du volcanisme de l'Afar et de la mégastructure Mer Rouge-Afar-Golfe d'Aden. Implications pétrogénétiques et géodynamiques. Bull. Soc. geol. Fr.VII série, 22, 945-957.

- Joron, J.L., Treuil, M., Jaffrezic, H. & Villemant, B. 1980b. Etude géochimique des éléments en traces dans les séries de roches volcaniques du rift d'Asal. Identification et analyse des processus d'accrétion. Bull. Soc. geol. Fr., VII, 22, 851-861.
- Le Bas, M., Le Maitre, R., Streckeisen, A. & Zanettin, B. 1986. A chemical classification of volcanics rocks based on total alkalin-silica diagram. J. Petrol., 27,3, 745-750.
- Le Gall B., Daoud, M.A., Rolet, J., Maury, R.C., Guillou, H. & Sue, C. Magma-driven anti-form structures in the Afar rift : the Ali Sabieh range, Djibouti. J. Struct. Geol., in press.
- Lépine, J. C., Ruegg, J.C. & Anis, A. M. 1980. Sismicité du rift d'Asal-Ghoubbet pendant la crise sismo-volcanique de novembre 1978. Bull. Soc. geol. Fr., XXII, 6, 809-816.
- Lépine, J. C. & Hirn, A. 1992. Seismotectonics in the Republic of Djibouti, linking the Afar Depression and the Gulf of Aden. Tectonophysics, 209, 65-86.
- Leroy, S., Gente, P. & 10 others, 2004. From rifting to drifting in the eastern Gulf of Aden: A complete margin survey coverage of a young oceanic basin from margin to margin. Terra Nova, 16, 185-192.
- Manighetti, I., Tapponnier, P., Courtillot, V., Gruszow, S. & Gillot., P.Y. 1997. Propagation of rifting along the Arabia-Somalia plate boundary: the Gulf of Aden and Tadjoura. J. Geophys. Res., 102, 2681-2710.
- Manighetti, I., Tapponnier, P., Gillot, P.Y., Jacques, E., Courtillot, V., Armijo, R., Ruegg, J.C. & King, G. 1998. Propagation of rifting along the Arabia-Somalia plate boundary into Afar. J. Geophys. Res., 103, 4947-4974.
- Manighetti, I., King, G.C.P., Gaudemer, Y., Scholz, C. & Doubre, C. 2001. Slip accumulation and lateral propagation of active normal faults in Afar. J. Geophys. Res., 13, 667-696.
- Marinelli, G. & Varet, J. 1973. Structure et évolution du Sud «Horst Danakil». C. R. Acad. Sc. Paris, 276, 1119-1122.
- Richard, O. 1979. Etude de la transition dorsale océanique – rift émergé: le Golfe de Tadjoura (République de Djibouti). Approche géologique, géochronologique et pétrologique. Thèse de 3ème cycle, Univ. Paris XI-Orsay, 149 pp.
- Rogers, N.W. 2006. Basaltic magmatism and the geodynamics of the East African Rift System. In: Yirgu, G., Ebinger, C.J., & Maguire, P.K.H. (Eds.), The Afar volcanic province within the East African Rift System. Geol. Soc. London, Sp. Pub., 259, 77-93.
- Ruegg, J.C., Lépine, J.C. & Vincent, C. 1980. Sismicité et micro-sismicité de la dorsale de Tadjoura, tectonique et frontière de plaques. Bull. Soc. géol. Fr., 22, 917-923.
- Schlische, R.W., Young, S.S., Ackermann, R.V. & Gupta, A. 1996. Geometry and scaling relations of a population of very small rift-related normal faults. Geology, 24, 683-686.
- Soliva, R., Schultz, R.A. & Benedicto, A. 2005. Three-dimensional displacement-length scaling and maximum dimension of normal faults in layered rocks. Geophys. Res. Lett., 32(6302), doi:10.1029/2005GL23007.
- Steiger, R.H. & Jäger, E., 1977. Subcommission on geochronology: convention on the use of decay constants in geo- and cosmochronology. Earth Planet. Sci. Lett., 36, 359-362.

Magmatism in the ocean basins. Geol. Soc. London Sp. Pub., 42, 313-345.

- Tamsett, D. & Searle, R.C. 1988. Structure and development of the midocean ridge plate boundary in the Gulf of Aden: Evidence from GLORIA side-scan sonar. J. Geophys. Res., 93, 3157-3178.
- Trudgill, B.D. & Cartwright, J.A. 1994. Relay ramp morphology and normal fault linkages, Canyonland National Park, Utah. Geol. Soc. Am. Bull., 106, 1143-1157.
- Vétel, W. & Le Gall, B. 2006. Dynamics of prolonged continental extension in magmatic rifts: the Turkana Rift case study (North Kenya). In: Yirgu, G., Ebinger, C.J. & Maguire, P.K. (Eds), The Afar volcanic province within the East African rift system. Geol. Soc. London. Sp. Pub., 259, 209-233.
- Vidal, P., Deniel, C., Vellutini, P.J., Piguet, P., Coulon, C., Vincent, J. & Audin, L. 1991. Changes of mantle sources in the course of a rift evolution: the Afar case. Geophys. Res. Lett., 18, 1913-1916.
- Vigny, C., de Chabalier, J.B., Ruegg, J.C., Huchon, P., Feigl, K., Cattin, R., Asfaw, L. & Khanbari, K. 2007. Twenty-five years of geodetic measurements along the Tadjoura-Asal rift system, Djibouti, East Africa. J. Geophys. Res., 112, B06410, doi:10.129/2004JB003230.
- Walsh, J.J. & Watterson, J. 1988. Analysis of relationship between displacement and dimensions of faults. J. Struct. Geol., 10, 239-247.
- Watterson, J. 1986. Fault dimensions, displacement and growth. Pure and Applied Geophysics, 124, 365-374.
- Wijns, C., Weinberg, R., Gessner, K. & Moresi, L. 2005. Mode of crustal extension determined by rheological layering. Earth Planet. Sci. Lett., 236, 120-134.
- Wojtal, S. F. 1994. Fault scaling laws and the temporal evolution of fault systems. J. Struct. Geol., 18, 265-280.
- Yurtmen, S., Guillou, H., Orhan, O., Rowbotham, G. & Westaway, R., 2002. Rate of strike-slip on the Amanos Fault (Karasu Valley, southern Turkey) constrained by K-Ar dating and geochemical analysis of Quaternary basalts. Tectonophysics, 344, 207-246.
- Ziegler, P.A. & Cloething, S. 2004. Dynamic processes controlling evolution of rifted basins. Earth Sci. Rev., 64, 1-50, doi :10.1016/50012-8252(03)00041-2.
- Zumbo, V., Féraud, G., Vellutini, H., Piguet, P. & Vincent, J. 1995. First 40Ar/39Ar datings on Early Pliocene to Plio-Pleistocene magmatic events of the Afar – Republic of Djibouti. J. Volc. Geoth. Res., 65, 281-295.